Computational and Theoretical Chemistry 996 (2012) 125–131

Contents lists available at SciVerse ScienceDirect

Computational and Theoretical Chemistry

journal homepage: www.elsevier.com/locate/comptc

Structural determination of $(Al_2O_3)_n$ (n = 1–7) clusters based on density functional calculation

Rong Li, Longjiu Cheng *

School of Chemistry and Chemical Engineering of Anhui University, Hefei, Auhui 230039, People's Republic of China

ARTICLE INFO

Article history:
Received 13 February 2012
Received in revised form 7 May 2012
Accepted 20 July 2012
Available online 27 July 2012

Keywords:
Alumina clusters
Genetic algorithm
Gas phase clusters
Global optimization
Density functional theory

ABSTRACT

We obtained the geometrical structures of $(Al_2O_3)_n$ (n = 1–7) clusters via genetic algorithm plus density functional theory method. Benchmark calculations show that the B3LYP/6-311 + G* method is reliable compared to CCSD(T)/aug-cc-pVTZ. However, the basis sets have great effect on relative energies of different structures. The global minimum structures are kite-shaped, cage and tea-cozy in structure for n = 1, 2 and 3 respectively, disordered at n = 4 and 5. At n = 6 and 7, a number of lower-energy isomers are obtained compared to the most stable structures obtained by Rahane et al. (J. Phys. Chem. C 115 (2011) 18111–18121). With increasing cluster size, structures show preference of disorder and some new configurations are derived.

1. Introduction

In bulk, alumina occurs in several different polymorphs due to the variety of packing modes for Al and O atoms, such as α-alumina, β-alumina, γ-alumina and θ-alumina, in which the valence electrons of Al atoms are transferred to the O atoms consequently producing close-shell Al trications and O dianions [1]. The most stable isomer is α-alumina among these multiple configurations, which is the main component of corundum. In the crystal lattice of α-Al_2O_3, O ions form a hexagonal close-packed structure with aluminum ions filling the octahedral sites. O ions are nearly face-centered cubic close-packed with the tetrahedral and octahedral sites being irregularly filled with Al ions in the phase of γ-alumina. Due to high melting and boiling point, α-Al_2O_3 is widely used as flame retardants and refractory materials. Because of pores and strong adsorption properties, γ-alumina is utilized in catalysts and adsorbents.

Alumina clusters are intermediates in size between molecules and bulk solids. They are of significant interest in atmospheric chemistry [2] and solid catalysts [3] because of their reduced size. Research has suggested that the gas-phase clusters and bulk of alumina are substantially different in structure. The isomer with D_{3d} symmetry for $(Al_2O_3)_4$ was presumed to be the global minimum and it was also used as a model for the bulk and surface of α-alumina [4–8]. However, Sierka et al. [9] proved that neither the bulk-like nor the caged structure is the global minimum by experiments and theoretical computation. In 2003, Heijnsbergen et al. [10] discovered the large abundance of $AlO{\cdot}(Al_2O_3)_{15}$ cluster cation in the mass spectrum of gas phase aluminum oxide clusters, which stands comparison with that of C_{60}. However, the structure has not been determined so far because of searching a structure with large size for $AlO{\cdot}(Al_2O_3)_{15}$ clusters being beyond the current computing ability. In comparison, many studies on structures of alumina clusters with small size have been performed by different methods [1,11–14]. Sun et al. [15] constructed the structures of $(Al_2O_3)_n$ with n = 1–10, revealing that cage structures are the global minimum at n = 1–5, cage-dimer structures at n = 6–9. Woodley [16] obtained the structures of $(Al_2O_3)_n$ with n = 1–5 by density functional theory (DFT), where the initial structures are located by an evolutionary algorithm with an interatomic potential. Rahane et al. [17] derived the structures of $(Al_2O_3)_n$ with n = 5–10 using DFT simulated annealing.

Although a mass of investigations on alumina clusters have been performed, some problems have not been resolved, for instance, the mechanism of structural transformations from small molecular clusters towards bulk solids is still not clear. So it is necessary to make a systematic research. In this paper, we obtained the structures of $(Al_2O_3)_n$ (n = 1–7) clusters by performing an unbiased global search of the DFT potential energy surface with genetic algorithm (GA) [18–20]. Most of structures are consistent with those obtained by Woodley [16] at n = 1–5 and some new low-energy isomers are reported. At n = 6 and 7, a number of new structures are located, which are lower in energy than the ones reported by Rahane et al. [17].

* Corresponding author. Tel./fax: +86 551 5107342.
E-mail address: clj@ustc.edu (L. Cheng).

2210-271X/$ - see front matter © 2012 Elsevier B.V. All rights reserved.
http://dx.doi.org/10.1016/j.comptc.2012.07.027

2. Computational details

2.1. Global optimization method

To have a systemic study of $(Al_2O_3)_n$ clusters, the cluster genetic algorithm (GA) was employed to search the potential energy surface directly using DFT method. All DFT computations were accomplished by the GAUSSIAN 09 package [21] using the hybrid B3LYP [22–24] functional. Our cluster GA-DFT method can be summarized as follows:

(a) Randomly generate *npop* structures to form the starting population of GA. Relax each structure in the population via DFT method at the B3LYP/6-31G*//B3LYP/3-21G level with a loose convergence criterion.
(b) For *k*-th iteration, randomly choose two structures from the population and perform Deaven–Ho crossover [19] to generate one child structure. After mutation, relax the child structure via DFT method at the B3LYP/6-31G*//B3LYP/3-21G level with a loose convergence criterion (10^{-4}). Input the relaxed structure to the structural bank. Update the population based on similarity [25] and energy.
(c) Increase *k* by 1. If *k* reaches a presetting number, terminate current calculation. Otherwise, go to step (b).

GA cannot promise to find the global minimum structure in one calculation, so for each case, five independent GA runs are carried out and the relaxed structures are recorded in one structural bank. The energetic sequences of the isomers may change at higher level DFT method, so a large population size is used and as many as low-lying isomers in the structural bank are considered. For example, in the optimization of $(Al_2O_3)_5$, the population size is 100, and the maximum iteration number is 2000. The rate of hitting the global minimum structure is 3/5. Then the top 200 lowest-energy B3LYP/6-31G*//B3LYP/3-21G isomers are resorted by the single point energy of high level B3LYP/6-311 + G*. Finally, the top 50 lowest-energy isomers are fully relaxed at B3LYP/6-311 + G* level of theory. Although the basis set affects the energetic sequences greatly, the top 10 lowest-energy B3LYP/6-311 + G* isomers are all involved in the top 100 B3LYP/6-31G*//B3LYP/3-21G isomers.

2.2. Benchmark calculations

To verify the reliability of the B3LYP functional, taking $(Al_2O_3)_2$ as a test case, in Table 1, we compared the relative energies calculated by various functionals (B3LYP, TPSSh [26], PBE0 [27], BP86 [28,29], M06 [30], BPW91 [31]) and the high-level CCSD(T) (coupled-cluster method with single, double and perturbative triple excitations) [32] method. It can be seen that, the gaps of different functionals are small (less than 0.26 eV) and B3LYP/6-311 + G* method is reliable compared to CCSD(T)/aug-cc-pVTZ method (within 0.08 eV). Gaps of the relative energies between 2C and 2D in different methods are higher than that of 2A and 2B, but the gap between B3LYP/6-311 + G* and CCSD(T)/aug-cc-pVTZ methods is also acceptable (~0.1 eV).

Table 1
Comparison of computed energies for low-lying isomers of $(Al_2O_3)_2$ (Fig. 2)[a].

Method	2A	2B	2C	2D
B3LYP	−1421.797590	0.48	1.19	1.20
TPSSh	−1421.768518	0.33	1.31	1.03
BP86	−1421.802678	0.37	1.13	1.05
PBE0	−1420.788664	0.34	1.30	1.06
M06	−1421.480235	0.59	1.35	1.27
BWP91	−1421.681001	0.37	1.13	1.04
CCSD(T)[b]	−1419.382902	0.40	1.23	1.13

[a] Energies for 2A are in atomic unit, other energies are relative to this in eV. Results are single point energies with 6-311 + G* basis set for the B3LYP/6-311 + G* geometry.
[b] The basis set is aug-cc-pVTZ for CCSD(T).

3. Results and discussion

Using the combination of GA and DFT, we obtained a series of structures for $(Al_2O_3)_n$ (n = 1–7) clusters at B3LYP/6-311 + G* level. The low-lying isomers are shown in Figs. 1–5. The relative energy and geometrical parameters of structures are available in the supplementary information. Most of structures in our results are consistent with those reported by Woodley [16] at n = 1–5, but a number of lower-energy isomers are derived at n = 6 and 7. In the following we will discuss the geometrical structures in detail.

3.1. Structures of $(Al_2O_3)_n$ (n = 1–7) clusters

$(Al_2O_3)_n$ (n = 1–3): As shown in Fig. 1, the global minima for n = 1, 2, and 3 are kite-shaped, cage and tea-cozy respectively. For Al_2O_3, the kite-shaped isomer (1A) is a triple state with C_{2v} symmetry, which is also reported in Ref. [33]. The liner isomer (1B) is 0.1 eV higher in energy with shorter Al–O bond lengths. For $(Al_2O_3)_2$, the global minimum (2A) is a cage with T_d symmetry agreeing with that of Sun et al. [15]. 2B is 0.49 eV higher in energy than 2A, in which four O and two Al atoms forming a planar linking two AlO units. It is also a low-lying isomer of $(Fe_2O_3)_2$ clusters [34]. Our results are in agreement with Woodley [16] in the top three isomers, but 2B is ranked first in their work. For $(Al_2O_3)_3$, the top four isomers are nearly degenerate in energy. 3A is a tea-cozy structure with C_1 symmetry and is also the global minimum of $(Fe_2O_3)_3$ clusters [34]. Our results are in agreement with Woodley [16] in the five lowest-energy isomers with difference only in the order of 3C and 3E.

$(Al_2O_3)_4$: 20 isomers are plotted in Fig. 2, in which the top 11 isomers are within 0.5 eV. The global minimum (4A) is formed by three 4-membered rings interconnected with an AlO_3 unit connecting the 4-membered rings from above and below, which is first reported by Sierka et al. [9] and is also the global minimum of $(Fe_2O_3)_4$ clusters [34]. 4B is 0.12 eV higher in energy, which can be considered as 3B added by one Al_2O_3 unit. The superimposed isomer (4C) that was assumed to be the global minimum is 0.19 eV higher in energy than 4A. The top three isomers are consistent with the low-energy structures in Ref. [16], but 4C is taken as the global minimum in that work. 4D, 4E and 4F are nearly degenerate in energy with C_1 symmetries. The cage isomer (4G) that is reported to be the global minimum in Ref. [15] is 0.37 eV higher in energy than 4A. 4H is a chiral structure with C_3 symmetry, which is 0.37 eV higher in energy. 4T that is a low-energy isomer in Ref. [16], becomes now 1.3 eV higher in energy than 4A.

$(Al_2O_3)_5$: 21 isomers are plotted in Fig. 3, in which the first 20 isomers are within 0.4 eV. The global minimum (5A) is a low-symmetry structure. The hat-like isomer (5C) with C_{3v} symmetry is 0.08 higher in energy than 5A. 5A and 5C are consistent with the first two structures of Woodley [16]. 5B is a newly located structure being 0.06 eV higher in energy than 5A, which has a fraction of a hat-like structure. The global minimum in Ref. [17] is only the seventh configuration (5G) being 0.23 eV higher in energy than 5A. 5D and 5E are disordered with 0.11 and 0.12 eV higher in energy than 5A respectively. The cage-like structure is not found in the global optimization procedure due to its high energy (1.27 eV higher in energy than 5A).

$(Al_2O_3)_6$: 18 low-lying isomers within 0.5 eV are plotted in Fig. 4. Both 6A and 6B are the lowest-lying isomers with nearly

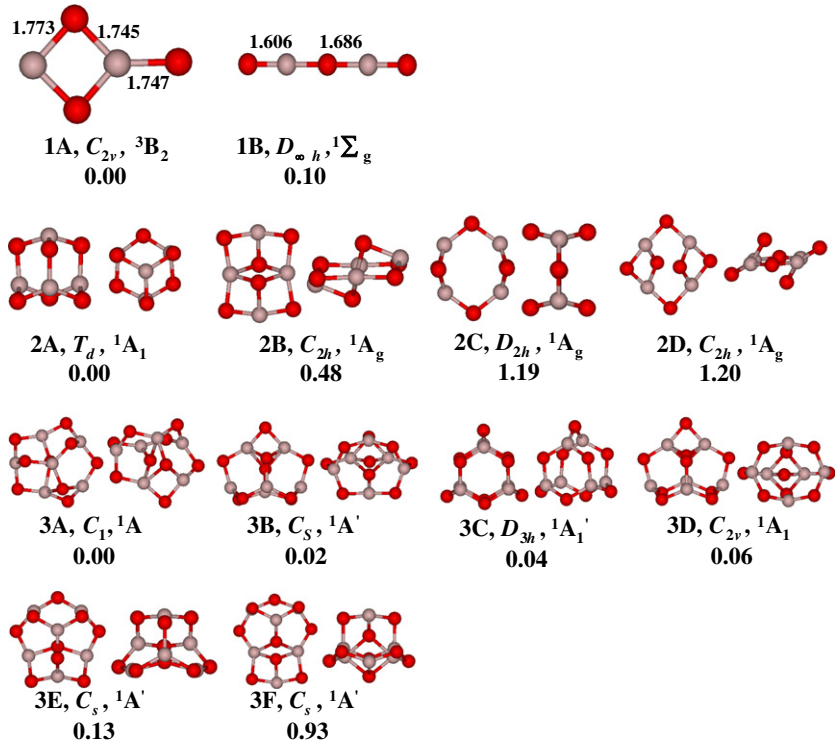

Fig. 1. Structures, symmetry point groups, electronic states and relative energies (eV) of the global minimum and lower-lying structures of $(Al_2O_3)_{1-3}$ at B3LYP/6-311 + G* level. For Al_2O_3, the bond lengths in angstrom are given. Al gray, O red.

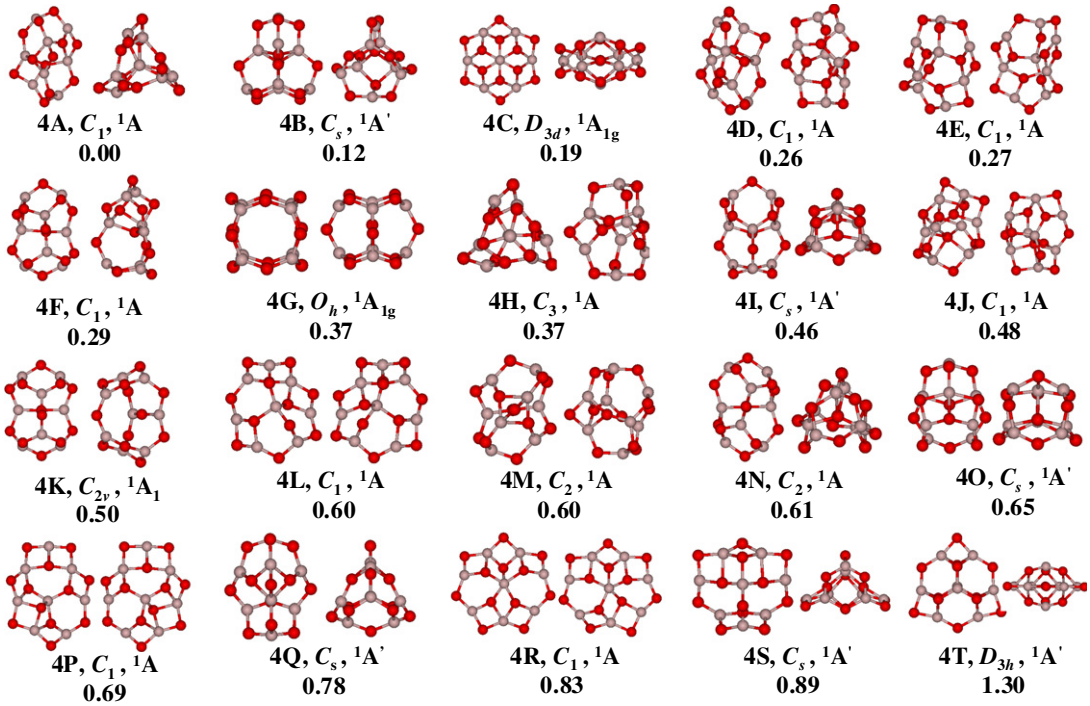

Fig. 2. Structures, symmetry point groups, electronic states and relative energies (eV) of the global minimum and lower-lying structures of $(Al_2O_3)_4$ at B3LYP/6-311 + G* level. Al gray, O red.

identical energies. 6A has a bottom of five 6- and one 4-membered rings, which consists of one Al_3O_4 unit. 6B has two tetrahedrons connected by two 'V-shaped' O–Al–O–Al–O patterns. The most stable structure reported by Rahane et al. [17] is only the 13th isomer (6M) in our results, which is 0.43 eV higher in energy than 6A. 6C is a low-symmetry structure, which consists of one Al_3O_4 unit. 6D has a bottom of 6-, 4- and 8-memdered rings with one Al_3O_4 unit, which is 0.11 eV higher in energy with C_s symmetry. 6E is a

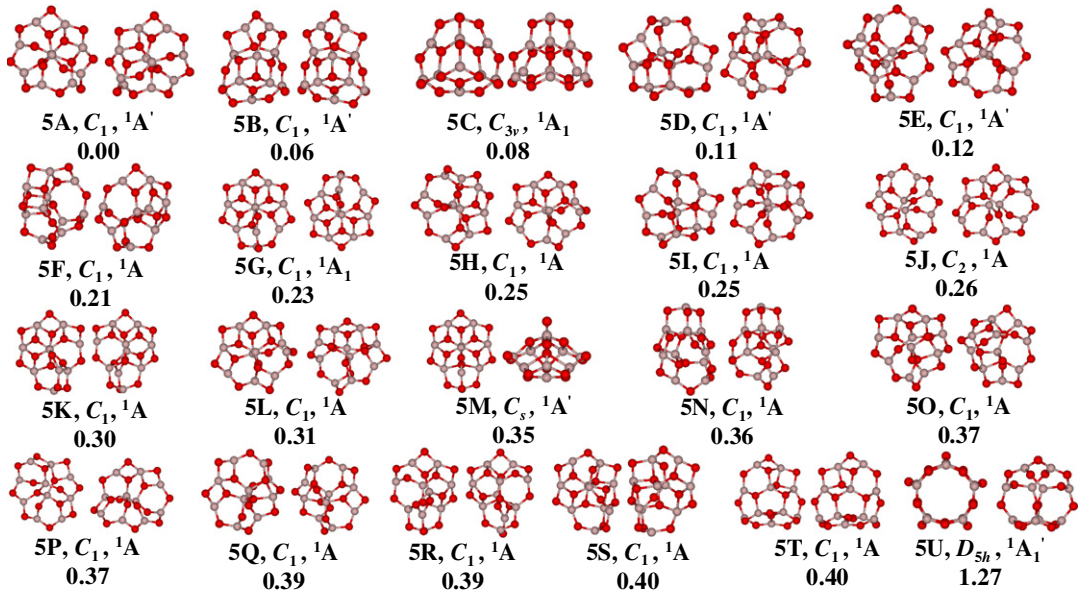

Fig. 3. Structures, symmetry point groups, electronic states and relative energies (eV) of the global minimum and lower-lying structures of $(Al_2O_3)_5$ at B3LYP/6-311 + G* level. Al gray, O red.

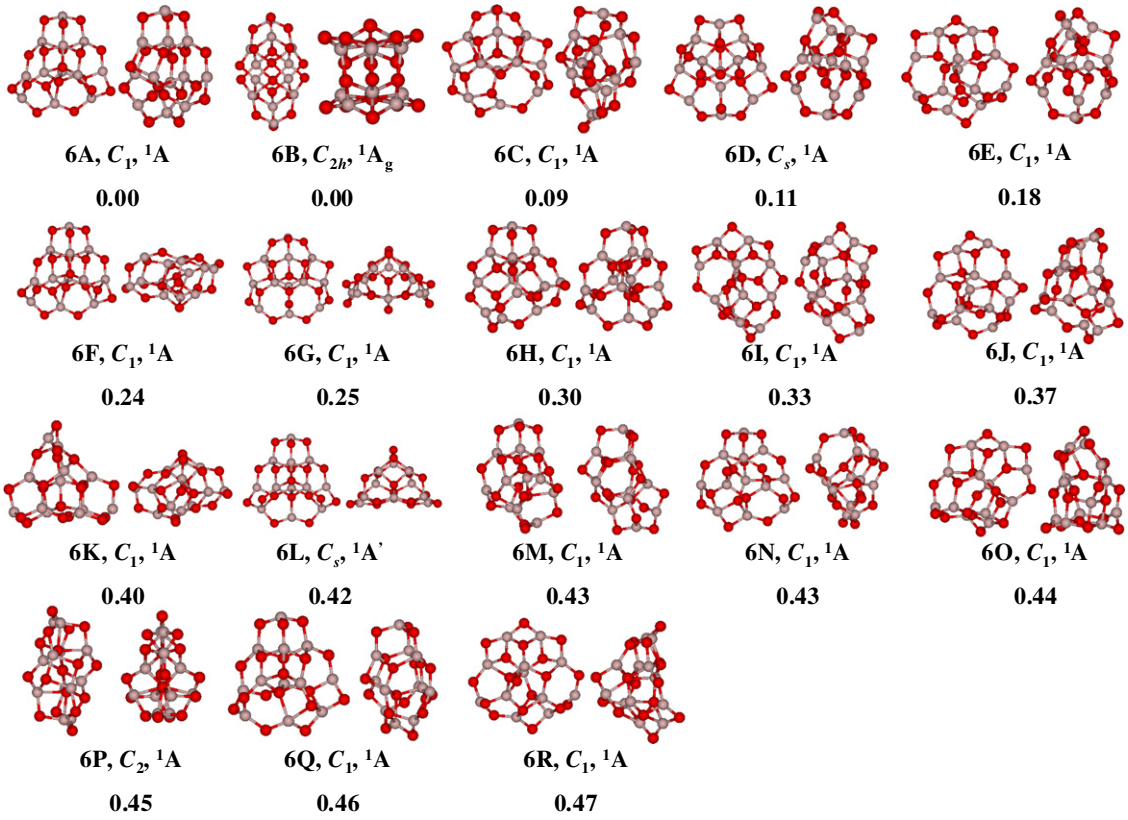

Fig. 4. Structures, symmetry point groups, electronic states and relative energies (eV) of the lower-lying structures of $(Al_2O_3)_6$ at B3LYP/6-311 + G* level. Al gray, O red.

low-symmetry structure, which is 0.18 eV higher in energy. 6F is similar to 6A in structure with 0.24 eV higher in energy. 6G is similar to 6C in atomic packing.

$(Al_2O_3)_7$: 14 low-lying isomers within 0.5 eV are plotted in Fig. 5. The most stable isomer (7A) has a bottom of 4-, 6- and 8-membered rings, which connect other three 4-membered rings that are each linked to the two other 4-membered rings by one Al and one O vertex. 7G that is reported to be the most stable isomer in Ref. [17] becomes now 0.38 eV higher in energy. The second isomer (7B) with C_1 symmetry can be considered as 6L added by an Al_2O_3 unit, which is 0.22 eV higher in energy than 7A. 7C is a low-symmetry structure being 0.24 eV higher in energy than 7A. 7D belongs to C_2 symmetry with 0.25 eV higher in energy. 7E can be considered as 4C added by three Al_2O_3 units, and is 0.31 eV higher

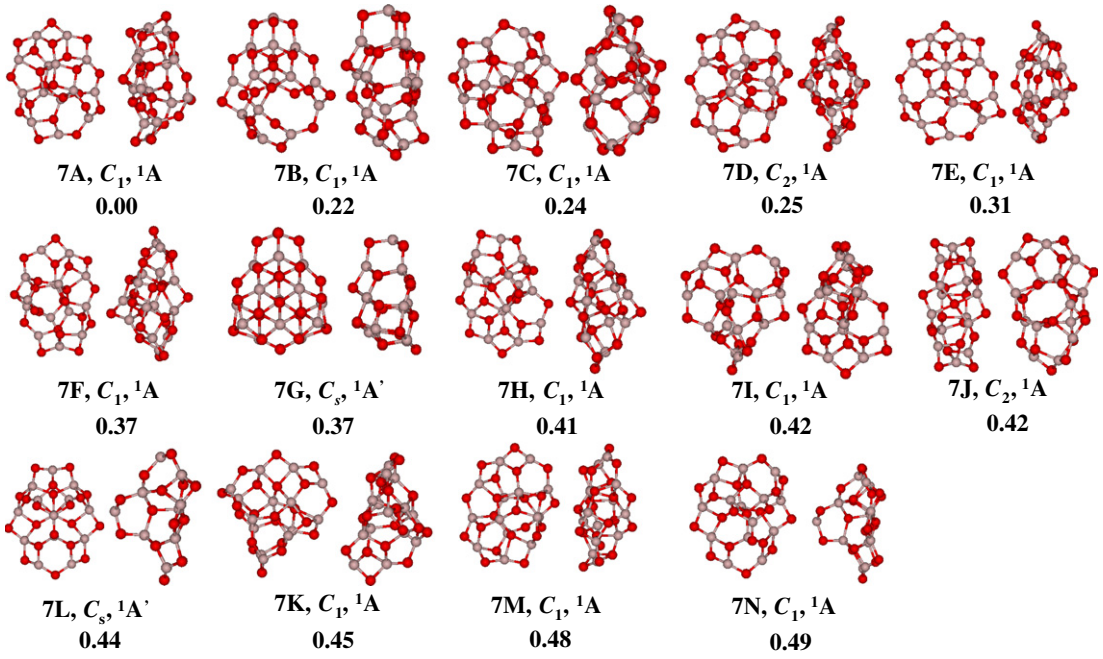

Fig. 5. Structures, symmetry point groups, electronic states and relative energies (eV) of the lower-lying structures of $(Al_2O_3)_7$ at B3LYP/6-311 + G* level. Al gray, O red.

in energy than 7A. 7F is similar to 7A in atomic packing. Other isomers are 0.4 eV higher in energy with C_1 symmetries (except for 7 J with C_2 symmetry).

3.2. The effects of basis sets on the relative stability

Although most of structures for $(Al_2O_3)_{1-5}$ are consistent with those reported by Woodley [16], the energetic sequences of various isomers are significantly different from ours. The benchmark calculations show that the effects of different functionals on the relative energy are very small. One may wonder if the basis sets affect the energetic sequences. For this reason, we took $(Al_2O_3)_4$ clusters as a test case and the relative energies at the 6-311 + G*, 6-31G*, 3-21G and STO-3G basis sets with the B3LYP functional are shown in Fig. 6. It is visible that the basis sets show great impact on the relative energies of various structures, e.g., the energy gaps between 4C and 4G are about 0.18, 0.45, 2.58, and 8.59 eV at the 6-311 + G*, 6-31G*, 3-21G and STO-3G basis sets respectively. The isomers (4 J, 4P, 4R and 4T) containing more 4-membered rings with more Al–O bonds are relatively lower in energy at small basis sets. While the isomers with less 4-membered rings (4B, 4K, 4M and 4Q) and the fullerene-like structure (4G) are higher in relative energy at small basis sets. 4C is indeed the global minimum for $(Al_2O_3)_4$ at small basis sets, which agrees with the previous studies, but it is not the lowest-energy structure at large basis sets possibly because the repulsion between the nearest same atoms (O–O and Al–Al in the 4-membered rings) is undervalued at small basis sets.

3.3. Comparison of cage and non-cage structures

Sun et al. [15] summarized that the fullerene-like structures of $(Al_2O_3)_n$ (n = 1–5) clusters are the global minima. However, some previous studies [9,13,17] suggested that cage-like structures are not stable. Our results also suggest that the fullerene-like structures are increasingly unstable with the increase of cluster size and are global minimum only at n = 2. To qualitatively interpret the instability of cage structures, we made a comparative study for the lowest-energy non-cage and cage structures at n = 2–5.

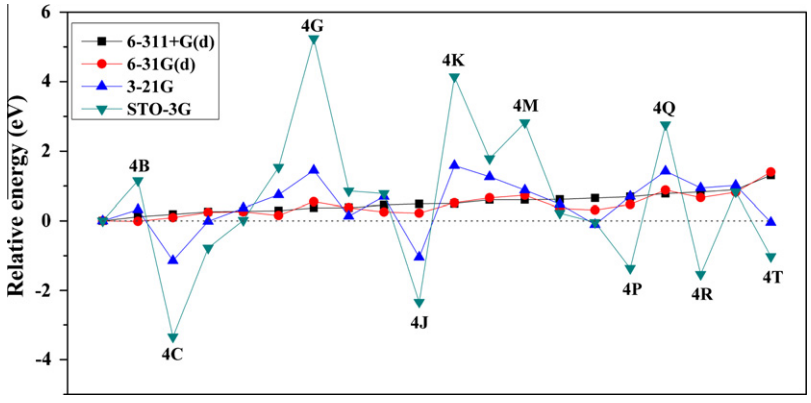

Fig. 6. Relative energies of the isomers for $(Al_2O_3)_4$ of B3LYP functional with various basis sets, STO-3G, 3-21G, 6-31G*, and 6-311 + G*. The energy of the first structure (4A) is taken as zero (base line) under each basis set, where a negative value indicates that the geometry is more stable than 4A under such a base set, and a positive value means that the geometry is unstable.

The binding energies were calculated by $E_b = [(2nE(Al) + 3nE(O_2/2) - E(A_{2n}O_{3n})]/n$. From Fig. 7a, it can be seen that the binding energy increases with increasing cluster size. Fig. 7b exhibits the tendency of relative stability of cage structures revealing that cage structures are increasingly instable with increasing cluster sizes. Fig. 7c compares the number Al–O bonds for non-cage and cage structures. Obviously, non-cage structures have more bonds and the gap of bond number increases with the further increase of cluster size compared to the cage structures.

3.4. Discussion

Nucleus-independent chemical shifts (NICS) value [35] is a popular measurement for aromaticity. To quantitatively analyze the aromaticity, Table 2 gives the NICS values in the cage centers of the cage structures. The NICS value for 2A (T_d cage) is only −1.44 ppm demonstrating that 2A shows very little aromaticity (as a comparison, the NICS value of benzene is −7.91 ppm). The NICS values for 3C (D_{3h} cage), 4C (D_{3d} cage), 4G (O_h cage) and 5T (D_{5h} cage) are −0.10, −0.95, −0.35, and −0.34 ppm respectively, which suggests that these cage structures are non-aromatic. Aromaticity is one of the reasons which results in the stability of cage structures and the cage alumina clusters are unstable because of non-aromaticity.

Alumina clusters are similar to iron oxide clusters not only because they have the same metal to oxygen ratio (2:3) but also because as bulk solids [34]. In order to study relative stability of cage alumina and iron oxide clusters, we make a comparison in relative energy. The energetic gap of the lowest-energy cage and non-cage isomers is −0.01, 0.33, 0.83, and 0.99 eV, respectively, for $(Fe_2O_3)_n$ clusters [34] and −0.48, 0.04, 0.37, and 1.27 eV, respectively, for $(Al_2O_3)_n$ clusters at $n = 2$–5. Meanwhile, it can be seen that the cage structures for iron oxide clusters are relatively more unstable than that for alumina clusters at $n = 2$–4. However, the gap of cage and non-cage isomers for alumina clusters (1.27 eV) is greater than that for iron oxide clusters (0.99 eV) at $n = 5$. The located lowest-energy structure at $n = 5$ may not be the real global minimum due to the difficulty of computation, and the low-lying isomers of $(Al_2O_3)_5$ may also be the global minimum of $(Fe_2O_3)_5$. Cage structures for alumina clusters are instable, however, they are relatively more stable than those of iron oxide clusters.

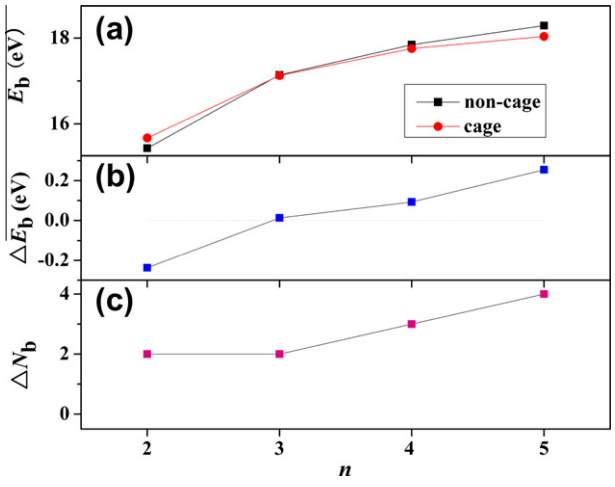

Fig. 7. (a) Binding energies (E_b) for the noncage and cages structures of $(Al_2O_3)_n$ ($n = 2$–5), where $E_b = [(2nE(Al) + 3nE(O_2/2) - E(A_{2n}O_{3n})]/n$. (b) The gap of binding energies for the noncage and cage structures. The gap is defined by $\Delta E_b = E_b$(global minimum) − E_b(cage). (c) The difference of the number of Al–O bonds for the noncage and cage structures. The difference is clarified by $\Delta N_b = N_b$(global minimum)-N_b(cage).

Table 2
The NICS values in cluster centers of cage $(Al_2O_3)_n$ clusters ($n = 2$–5) and benzene at the B3LYP/6-311 + G* level.

Species	Symmetry	NICS
$(Al_2O_3)_2$	T_d	−1.44
$(Al_2O_3)_3$	D_{3h}	−0.10
$(Al_2O_3)_4$	D_{3d}	−0.95
$(Al_2O_3)_4$	O_h	−0.35
$(Al_2O_3)_5$	D_{5h}	−0.34
Benzene	D_{6h}	−7.91

4. Conclusions

Stoichiometric $(Al_2O_3)_n$ ($n = 1$–7) clusters are investigated theoretically via GA plus DFT. The global minimum structures are kite-shaped, cage and tea-cozy in structure for $n = 1$, 2 and 3 respectively, disordered at $n = 4$ and 5. At $n = 6$ and 7, twelve and six lower-energy isomers are found respectively compared to those obtained by Rahane et al. The structures show preference of disorder and many new configurations are found with increasing cluster size, in which some isomers are nearly degenerate in energy. Benchmark calculation demonstrates that the effects of various functionals on energetic sequences are small. However, the basis sets have great impact on the relative energies of various structures. It is proved that the D_{3d} cage (4C, seen as a fragment of α-alumina solid) is the lowest-energy structure of $(Al_2O_3)_4$ only at small basis sets. With increasing cluster size, it is expected that alumina clusters will also favor disorder at larger cluster sizes because of the degree of structural disorder increasing.

Acknowledgments

This work is financed by the National Natural Science Foundation of China (20903001), by the 211 Project and the outstanding youth foundation of Anhui University. The calculations are carried on the High-Performance Computing Center of Anhui university.

Appendix A. Supplementary material

Supplementary data associated with this article can be found, in the online version, at http://dx.doi.org/10.1016/j.comptc.2012.07.027.

References

[1] A. Martinez, L.E. Sansores, R. Salcedo, F.J. Tenorio, J.V. Ortiz, Al_3O_n and $Al_3O_n^-$ ($n = 1$–3) clusters: structures, photoelectron spectra, harmonic vibrational frequencies, and atomic charges, J. Phys. Chem. A 106 (2002) 10630–10635.
[2] R.P. Turco, O.B. Toon, R.C. Whitten, R.J. Cicerone, Space shuttle ice nuclei, Nature 298 (1982) 830–832.
[3] N. Magg, J.B. Giorgi, T. Schroeder, M. Baumer, H.-J. Freund, Model catalyst studies on vanadia particles deposited onto a thin-film alumina support. 1. Structural characterization, J. Phys. Chem. B 106 (2002) 8756–8761.
[4] M. Casarin, C. Maccato, A. Vittadini, Theoretical study of the chemisorption of CO on Al_2O_3(0001), Inorg. Chem. 39 (2000) 5232–5237.
[5] E.M. Fernandez, R. Eglitis, G. Borstel, L.C. Balbas, Adsorption and dissociation of water on relaxed alumina clusters: a first principles study, Phys. Status Solidi B 242 (2005) 807–809.
[6] A.K. Gianotto, J.W. Rawlinson, K.C. Cossel, J.E. Olson, A.D. Appelhans, G.S. Groenewold, Hydration of alumina cluster anions in the gas phase, J. Am. Chem. Soc. 126 (2004) 8275–8283.
[7] E.F. Sawilowsky, O. Meroueh, H.B. Schlegel, W.L. Hase, Structures, energies, and electrostatics for methane complexed with alumina clusters, J. Phys. Chem. A 104 (2000) 4920–4927.
[8] J.M. Wittbrodt, W.L. Hase, H.B. Schlegel, Ab initio study of the interaction of water with cluster models of the aluminum terminated (0001) α-aluminum oxide surface, J. Phys. Chem. B 102 (1998) 6539–6548.
[9] M. Sierka, J. Dobler, J. Sauer, G. Santambrogio, M. Brummer, L. Woste, E. Janssens, G. Meijer, K.R. Asmis, Unexpected structures of aluminum oxide clusters in the gas phase, Angew. Chem. Int. Ed. 46 (2007) 3372–3375.

[10] D. van Heijnsbergen, K. Demyk, M.A. Duncan, G. Meijer, G. von Helden, Structure determination of gas phase aluminum oxide clusters, Phys. Chem. Chem. Phys. 5 (2003) 2515–2519.
[11] A.B.C. Patzer, C. Chang, E. Sedlmayr, D. Sülzle, A density functional study of small Al_xO_y (x, y = 1–4) clusters and their thermodynamic properties, Eur. Phys. J. D. 32 (2005) 329–337.
[12] M.-M. Zhong, X.-Y. Kuanga, H.-Q. Wanga, H.-F. Li, Y.-R. Zhao, Density functional study of the structural and electronic properties of tetra-aluminum oxide $Al_4O_n^{\lambda}$ ($3 \leqslant n \leqslant 8$, $\lambda = 0, -1$) clusters, Mol. Phys. 109 (2011) 603–612.
[13] M. Sierka, J. Döbler, J. Sauer, H.-J. Zhai, L.-S. Wang, The $[(Al_2O_3)_2]^-$ anion cluster: electron localization–delocalization isomerism, Chem. Phys. Chem. 10 (2009) 2410–2413.
[14] E.F. Archibong, N. Seeburrun, P. Ramasami, Geometric and electronic structure of AlO_4 and AlO_4^-, Chem. Phys. Lett. 481 (2009) 169–172.
[15] J. Sun, W.C. Lu, W. Zhang, L.Z. Zhao, Z.S. Li, C.C. Sun, Theoretical study on $(Al_2O_3)_n$ (n = 1–10 and 30) fullerenes and H_2 adsorption properties, Inorg. Chem. 47 (2008) 2274–2279.
[16] S.M. Woodley, Atomistic and electronic structure of $(X_2O_3)_n$ nanoclusters; n = 1–5, X=B, Al, Ga, In and Tl, Proc. R. Soc. A 467 (2011) 2020–2042.
[17] A.B. Rahane, M.D. Deshpande, V. Kumar, Structural and electronic properties of $(Al_2O_3)_n$ clusters with n = 1–10 from first principles calculations, J. Phys. Chem. C 115 (2011) 18111–18121.
[18] B. Hartke, Global geometry optimization of clusters using genetic algorithms, J. Phys. Chem. 97 (1993) 9973–9976.
[19] D.M. Deaven, K.M. Ho, Molecular geometry optimization with a genetic algorithm, Phys. Rev. Lett. 75 (1995) 288–291.
[20] C. Roberts, R.L. Johnston, Investigation of the structures of MgO clusters using a genetic algorithm, Phys. Chem. Chem. Phys. 3 (2001) 5024–5034.
[21] M.J. Frisch, G.W. Trucks, H.B. Schlegel, G.E. Scuseria, M.A. Robb, J.R. Cheeseman, G.Scalmani, V. Barone, B. Mennucci, G.A. Petersson, H. Nakatsuji, M. Caricato, X. Li, H.P. Hratchian, A.F. Izmaylov, J. Bloino, G. Zheng, J.L. Sonnenberg, M. Hada, M. Ehara, K. Toyota, R. Fukuda, J. Hasegawa, M. Ishida, T. Nakajima, Y. Honda, O. Kitao, H. Nakai, T. Vreven, J.A. Montgomery, Jr., J.E. Peralta, F. Ogliaro, M. Bearpark, J.J. Heyd, E. Brothers, K.N. Kudin, V.N. Staroverov, R. Kobayashi, J. Normand, K. Raghavachari, A. Rendell, J.C. Burant, S.S. Iyengar, J. Tomasi, M. Cossi, N. Rega, J.M. Millam, M. Klene, J.E. Knox, J.B. Cross, V. Bakken, C. Adamo, J. Jaramillo, R. Gomperts, R.E. Stratmann, O. Yazyev, A.J. Austin, R. Cammi, C. Pomelli, J.W. Ochterski, R.L. Martin, K. Morokuma, V.G. Zakrzewski, G.A. Voth, P. Salvador, J.J. Dannenberg, S. Dapprich, A.D. Daniels, O. Farkas, J.B. Foresman, J.V. Ortiz, J. Cioslowski, D.J. Fox, Gaussian 09, revision B.01; Gaussian, Inc., Wallingford CT 2009.
[22] A.D. Becke, Density-functional thermochemistry. III. The role of exact exchange, J. Chem. Phys. 98 (1993) 5648–5652.
[23] C. Lee, W. Yang, R.G. Parr, Development of the Colle–Salvetti correlation-energy formula into a functional of the electron density, Phys. Rev. B 37 (1988) 785–789.
[24] B. Miehlich, A. Savin, H. Stoll, H. Preuss, Results obtained with the correlation energy density functionals of becke and Lee, Yang and Parr, Phys. Rev. Lett. 157 (1989) 200–206.
[25] L.J. Cheng, W.S. Cai, X.G. Shao, A connectivity table for cluster similarity checking in the evolutionary optimization method, Chem. Phys. Lett. 389 (2004) 309–314.
[26] J. Tao, J.P. Perdew, V.N. Staroverov, G.E. Scuseria, Climbing the density functional ladder: nonempirical meta-generalized generalized gradient approximation designed for molecules and solids, Phys. Rev. Lett. 91 (2003) 146401.
[27] C. Adamo, V. Barone, Toward reliable density functional methods without adjustable parameters: the PBE0 model, J. Chem. Phys. 110 (1999) 6158–6170.
[28] A.D. Becke, Density-functional exchange-energy approximation with correct asymptotic behavior, Phys. Rev. A 38 (1988) 3098–3100.
[29] J.P. Perdew, Density-functional approximation for the correlation energy of the inhomogeneous electron gas, Phys. Rev. B 33 (1986) 8822–8824.
[30] Y. Zhao, D.G. Truhlar, A new local density functional for main-group thermochemistry, transition metal bonding, thermochemical kinetics, and noncovalent interactions, J. Chem. Phys. 125 (2006) 194101.
[31] J.A. Chevary, S.H. Vosko, K.A. Jackson, M.R. Pederson, D.J. Singh, C. Fiolhais, Erratum: atoms, molecules, solids, and surfaces: applications of the generalized gradient approximation for exchange and correlation, Phys. Rev. B 48 (1993) 4978.
[32] Z. Cao, M. Duran, M. Solà, Low-lying electronic states and molecular structure of FeO_2 and FeO_2^-, Chem. Phys. Lett. 274 (1997) 567–575.
[33] C. Chang, A.B.C. Patzer, E. Sedlmayr, D. Sülzle, Ab initio studies of stationary points of the Al_2O_3 molecule, Eur. Phys. J. D 2 (1998) 57–62.
[34] X.L. Ding, W. Xue, Y.P. Ma, Z.C. Wang, S.G. He, Density functional study on cage and noncage $(Fe_2O_3)_n$ clusters, J. Chem. Phys. 130 (2009) 014303.
[35] P.v.R. Schleyer, C. Maerker, A. Dransfeld, H. Jiao, N.J.R.v.E. Hommes, Nucleus-independent chemical shifts: a simple and efficient aromaticity probe, J. Am. Chem. Soc. 118 (1996) 6317–6318.